Role of Quantum Coherence in Kinetic Uncertainty Relations

Kacper Prech[1,*] Patrick P. Potts[1] and Gabriel T. Landi[2]

[1]*Department of Physics and Swiss Nanoscience Institute, University of Basel, Klingelbergstrasse 82, 4056 Basel, Switzerland*

[2]*Department of Physics and Astronomy, University of Rochester, P.O. Box 270171, Rochester, NY, USA*

(Received 19 August 2024; accepted 18 December 2024; published 13 January 2025)

The kinetic uncertainty relation (KUR) bounds the signal-to-noise ratio of stochastic currents in terms of the number of transitions per unit time, known as the dynamical activity. This bound was derived in a classical context and can be violated in the quantum regime due to coherent effects. However, the precise connection between KUR violations and quantum coherence has so far remained elusive, despite significant investigation. In this Letter, we solve this problem by deriving a modified bound that exactly pinpoints how, and when, coherence might lead to KUR violations. Our bound is sensitive to the specific kind of unraveling of the quantum master equation. It, therefore, allows one to compare quantum jumps and quantum diffusion, and understand, in each case, how quantum coherence affects fluctuations. We illustrate our result on a double quantum dot, where the electron current is monitored either by electron jump detection or with continuous diffusive charge measurement.

DOI: 10.1103/PhysRevLett.134.020401

Introduction—Superposition is one of the key features of quantum mechanics that distinguishes it from classical physics. While the most prominent consequences of quantum coherence are entanglement and nonlocality [1–3], it also has a profound effect on dynamical properties, such as the fluctuations of currents in open quantum systems [4–6], and thermodynamic quantities such as heat and work [7–21]. Crucially, since these fluctuations depend on two-time correlations [22], this effect is not necessarily related to the amount of coherence present in a quantum state, but rather to the dynamical generation and consumption of coherence in a process. However, the precise way in which this takes place remains poorly understood.

In classical systems, current fluctuations are constrained by a set of bounds, discovered over the last decade, and collectively known as thermokinetic uncertainty relations [23–36]. They provide lower bounds on the noise-to-signal ratio D/J^2, where J is the average current, and D (called the noise, scaled variance, or diffusion coefficient) quantifies its fluctuations. Two prominent classes of bounds are the thermodynamic uncertainty relation (TUR) [25,26] and the kinetic uncertainty relation (KUR) [23,24]. This Letter will focus on the latter, which reads

$$\frac{D}{J^2} \geq \frac{1}{A}, \tag{1}$$

where A is the average dynamical activity ("freneticity") [37] and measures the average number of transitions per unit time in a stochastic system. The fact that the right-hand side depends on $1/A$ means that high dynamical activities are required in order to decrease fluctuations. The bound, therefore, has a very practical implication in establishing the minimum activity required to achieve a certain precision. The TUR has an analogous form to the KUR, but the bound is given in terms of the average entropy production rate in place of the dynamical activity, which is a measure of irreversibility.

In the quantum domain, however, Eq. (1) can be violated. Several authors have worked to pinpoint the precise mechanisms responsible for these violations [4–6,38–47]. While TUR violations received a considerable amount of attention, results for the KUR were first explored recently in [4]. It is noteworthy that quantum effects are not always beneficial for reducing fluctuations, and there are cases where it can actually be deleterious [40].

This, therefore, begs the question of when, and how, can coherence be used to improve the precision of stochastic currents? This led several authors to derive quantum extensions of the TUR and KUR [48–57]. These bounds are very useful in providing practical constraints. And they have also helped shed light on what new ingredients come into play when we move to the quantum domain. Unfortunately, they do not shed much light on the precise roles of coherence.

In this Letter we derive a new bound that holds for Markovian open quantum systems, in the presence of arbitrary quantum coherent effects. It replaces Eq. (1) with

$$\frac{D}{J^2} \geq \frac{(1+\psi)^2}{A}, \tag{2}$$

where $\psi \propto [\hat{H}, \hat{\rho}_{ss}]$ [c.f. Eq. (6)] is directly proportional to how much the steady-state density matrix $\hat{\rho}_{ss}$ fails to

*Contact author: kacper.prech@unibas.ch

commute with the system Hamiltonian $\hat{H}$ (i.e., to the amount of energetic coherence present in the steady state). We refer to Eq. (2) as the ψ-KUR. A nearly identical bound also holds for the diffusive unraveling, with $(1+\psi) \to (1/2+\psi)$. In diffusive measurements, instead of directly detecting each monitored transition, their outputs are combined with strong reference currents, and their deviations are observed [58,59]. For incoherent processes $\psi = 0$, and our result reduces to the classical KUR [Eq. (1)]. Conversely, for coherent processes, violations of Eq. (1) become possible when $\psi \in [-2, 0]$, while outside this interval violations are strictly not allowed. This, therefore, unambiguously pinpoints energetic coherence as the fundamental ingredient required for KUR violations. The inequality in Eq. (2) also uncovers the special case $\psi = -2$, in which the original KUR holds, even though the system has coherence. To illustrate the significance of this special point, as well as the intuition behind Eq. (2), we carry out a detailed analysis of a double quantum dot (DQD) model [60].

The ψ-KUR—We consider an open quantum system with a density matrix $\hat{\rho}_t$ that evolves in time according to the Lindblad master equation [61–64] ($\hbar = 1$)

$$\frac{d}{dt}\hat{\rho}_t = -i[\hat{H}, \hat{\rho}_t] + \sum_k D[\hat{L}_k]\hat{\rho}_t =: \mathcal{L}\hat{\rho}_t, \tag{3}$$

where $\hat{H}$ is the Hamiltonian of the system, $\hat{L}_k$ are Lindblad jump operators, and $D[\hat{O}]\hat{\rho}_t := \hat{O}\hat{\rho}_t\hat{O}^\dagger - \frac{1}{2}\{\hat{O}^\dagger\hat{O}, \hat{\rho}_t\}$. We assume the system has a unique steady state $\mathcal{L}\hat{\rho}_{\rm ss} = 0$.

The derivation of Eq. (2) is done in the Appendix. Here we only make explicit the main quantities involved. Our bound concerns generic stochastic counting observables and integrated currents $N(\tau)$, whose definition depends on the unraveling in question (specified below). The average and scaled variance (noise) of the stochastic current $I(\tau) = dN(\tau)/d\tau$ are given by

$$J = \frac{\mathrm{E}[N(\tau)]}{\tau}, \qquad D = \frac{\mathrm{Var}[N(\tau)]}{\tau}, \tag{4}$$

where $\mathrm{E}[\cdot]$ denotes the expectation value and $\mathrm{Var}[\cdot]$ the variance. The dynamical activity reads [48,49]

$$A = \sum_k \mathrm{Tr}\{\hat{L}_k\hat{\rho}_{\rm ss}\hat{L}_k^\dagger\} \tag{5}$$

and represents the average number of jumps per unit time in the steady state. In turn, the factor ψ in Eq. (2) is given by the expression

$$\psi = \frac{\mathrm{Tr}\{\mathcal{J}\mathcal{L}^+\mathcal{H}\hat{\rho}_{\rm ss}\}}{J}, \tag{6}$$

where $\mathcal{H}\hat{\rho} := -i[\hat{H}, \hat{\rho}]$, $\mathcal{L}^+$ is the Drazin inverse [65] of $\mathcal{L}$ (see Supplemental Material [66] for details), and $\mathcal{J}$ is the current superoperator, i.e., $J = \mathrm{Tr}\{\mathcal{J}\hat{\rho}\}$. We note that the superoperator $\mathcal{H}$ describes the amount of steady-state energetic coherence, whereas the Drazin inverse depends on the relaxation rates, highlighting that ψ depends on the dynamics.

Crucially, since ψ depends on $\mathcal{J}$, our bound is sensitive to both the particular current measurement and the type of unraveling. For the jump, unraveling the current superoperator is given by

$$\mathcal{J}\hat{\rho} = \sum_k \nu_k \hat{L}_k\hat{\rho}\hat{L}_k^\dagger, \tag{7}$$

where ν_k denotes the weight with which a jump $\hat{L}_k$ changes the integrated current $N(t)$ [22,58]. Conversely, for the diffusive unravelling [22,58]

$$\mathcal{J}_{\rm d}\hat{\rho} = \sum_k \nu_k \left(e^{-i\phi_k}\hat{L}_k\hat{\rho} + \hat{\rho}\hat{L}_k^\dagger e^{i\phi_k}\right), \tag{8}$$

where ϕ_k are arbitrary angles. In this case the bound Eq. (2) holds with the replacements $(1+\psi) \to (1/2+\psi)$, $\mathcal{J} \to \mathcal{J}_d$, and $J \to J_d$.

Having introduced the quantum ψ-KUR [Eq. (2)], we compare it with a different, previously obtained bound [48]:

$$\frac{D}{J^2} \geq \frac{1}{A+\chi}, \tag{9}$$

which also applies in the steady state for the quantum jump unraveling of the Lindblad master equation [Eq. (3)]. For the diffusive unraveling, 1 is replaced by 1/4 in the numerator. Here χ is a different coherence-dependent factor (see Supplemental Material [66] for the expression). However, as opposed to ψ, it does not concisely capture how much $\hat{\rho}$ fails to commute with $\hat{H}$. Moreover, for a given system, the factor χ is the same for all unravelings and current measurements, because it does not depend on the current superoperator $\mathcal{J}$, forfeiting a tailoring of the noise-to-signal bound to a particular current measurement. This is in contrast to ψ.

Double quantum dot—We illustrate the ψ-KUR [Eq. (2)] on a DQD model [60], where we find that $\psi \in [-2, 0]$ allows for considerable violations of the classical KUR due to coherence when the noise D cannot be faithfully described by a classical model. The system consists of left (L) and right (R) spinless quantum dots, which are weakly coupled to their respective fermionic reservoirs. The Hamiltonian is

$$\hat{H} = \sum_{\ell=L,R} \epsilon\hat{c}_\ell^\dagger\hat{c}_\ell + g\left(\hat{c}_L^\dagger\hat{c}_R + \hat{c}_R^\dagger\hat{c}_L\right), \tag{10}$$

where $\hat{c}_\ell$ ($\hat{c}_\ell^\dagger$) are annihilation (creation) operators of an electron in dot $\ell = L, R$, ϵ is the occupation energy of each

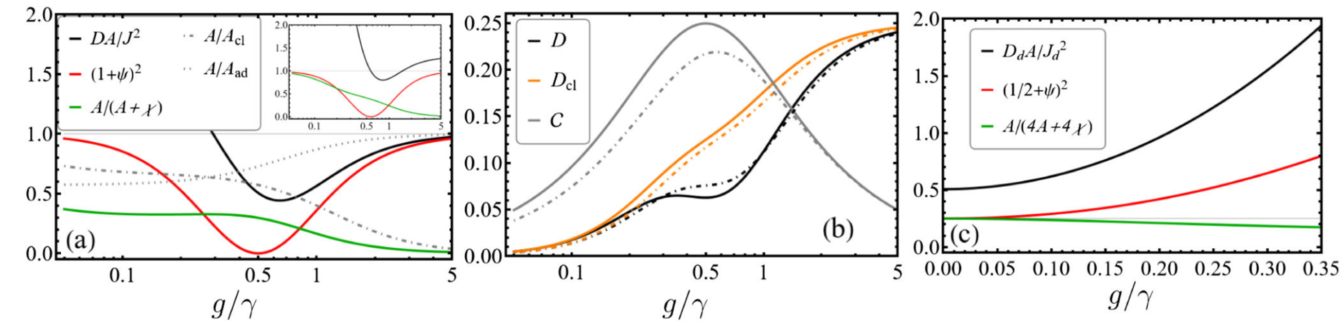

FIG. 1. ψ-KUR in the DQD. (a) Current fluctuations in the quantum jump unraveling as a function of g/γ, with $\gamma = \gamma_L = \gamma_R$ and no dephasing ($\Gamma = 0$): (black) DA/J^2; (red) $(1+\psi)^2$ [computed from Eq. (13)], which bounds the black curve according to Eq. (2); (green) $A/(A+\chi)$ from Eq. (9); (dashed gray) $A/A_{\rm cl}$; (dotted gray) $A/A_{\rm ad}$. Parameters: $\beta_L\mu_L = -\beta_R\mu_R = 7$ and $\epsilon = 0$. The inset shows the same plots with dephasing rate $\Gamma/\gamma = 0.3$. (b) The noise D as a function of g/γ for the quantum (black) and classical (orange) models, as well as the l_1 norm of coherence $\mathcal{C}$ (gray) obtained with Eq. (14). Solid lines correspond to the parameters of (a) (without dephasing) and dashed lines to those of the inset of (a) (with dephasing). (c) Same as (a) but for the diffusive measurement of the charge difference between the quantum dots. Parameters are the same as in (a), except $\Gamma/\gamma = 1$.

quantum dot, and g the coherent tunnel strength. The chemical potential, inverse temperature, and coupling strength to reservoir ℓ are denoted by μ_ℓ, β_ℓ, and γ_ℓ, respectively.

The Lindblad master equation governing the time evolution of the system is given by

$$\mathcal{L}\hat{\rho} = -i[\hat{H},\hat{\rho}] + \sum_\ell \mathcal{L}_\ell\hat{\rho} + \frac{\Gamma}{2}D[\hat{c}_L^\dagger\hat{c}_L - \hat{c}_R^\dagger\hat{c}_R]\hat{\rho}, \quad (11)$$

where the last term denotes a dephasing in the local basis, with strength Γ, while

$$\mathcal{L}_\ell\hat{\rho} = \gamma_\ell\Big(f_\ell D[\hat{c}_\ell^\dagger] + (1-f_\ell)D[\hat{c}_\ell]\Big)\hat{\rho} \quad (12)$$

describes the coupling to reservoir ℓ, with Fermi–Dirac occupation $f_\ell \coloneqq \{\exp[\beta_\ell(\epsilon-\mu_\ell)]+1\}^{-1}$.

For the quantum jump unraveling, we consider a net flow of electrons from the left reservoir through the system, which has the average current $J = \gamma_L \mathrm{Tr}[f_L\hat{c}_L^\dagger\hat{\rho}\hat{c}_L - (1-f_L)\hat{c}_L\hat{\rho}\hat{c}_L^\dagger]$. The analytical expression for ψ in this case reads

$$\psi = \frac{-2\gamma_L\gamma_R(\gamma_L+\gamma_R+2\Gamma)}{4g^2(\gamma_L+\gamma_R)+\gamma_L\gamma_R(\gamma_L+\gamma_R+2\Gamma)} < 0, \quad (13)$$

which ranges between $\psi = -2$ when $g \to 0$ and $\psi = 0$ when $g \to \infty$. It is, thus, always in the range $(1+\psi)^2 < 1$ such that, for this model, the DQD coherence always allows for a reduced minimal activity to sustain a fixed noise-to-signal ratio. Figure 1(a) compares DA/J^2 with $(1+\psi)^2$ as a function of g/γ. The bound is found to be tighter for large g/γ. Moreover, it is tighter than Eq. (9) for the majority of values g/γ, but not always.

The steady-state coherence, quantified by the l_1 norm [67] in the occupation basis, is (see Supplemental Material [66])

$$\mathcal{C} = \frac{2g|f_L - f_R|}{\gamma_L+\gamma_R+\Gamma}|\psi|. \quad (14)$$

Thus, the range of coherent tunnel strength g where ψ predicts a significant contribution of coherence to the KUR violation corresponds to the peak of coherence.

Dephasing (Γ) is found to be detrimental to loosening the KUR bound, and we find $(1+\psi)^2 \to 1$ in the strong Γ limit consistently with our expectations for incoherent dynamics. A similar, anticipated effect of dephasing, which features in the inset of Fig. 1(a), is that DA/J^2 obeys Eq. (1) in a much wider range of g/γ.

Breakdown of the classical description—To gain additional insights we ask whether the noise D can be captured by an effective classical model, where transport is described by a Markovian rate equation

$$\frac{d}{dt}\vec{p} = W\vec{p}, \quad (15)$$

where W is a matrix of transition rates and $\vec{p} = [p_0, p_L, p_R, p_D]$ is a vector of probabilities that the system is empty, occupied on the left, occupied on the right, or doubly occupied. The rates arising from the coupling to the environment are obtained from Eq. (12)—for instance, $W_{L0} = \gamma_L f_L$. Conversely, the coherent tunneling is replaced by the rate

$$W_{LR} = W_{RL} = \frac{4g^2}{\gamma_L+\gamma_R+2\Gamma}, \quad (16)$$

which can be obtained from perturbation theory [4,5,68] or by imposing that the two models should have the same average current.

Figure 1(b) compares the noise in the classical and quantum models. While the classical model describes the average current in the entire range of g/γ, there is a discrepancy in the noise D, which appears precisely where the coherence in Eq. (14) has a peak. In this regime, the classical model fails to reproduce the reduction of the noise predicted by the quantum master equation. This coincides with the range where $(1+\psi)^2 < 1$, i.e., where the ψ-KUR in Eq. (2) differs from the KUR in Eq. (1).

While the classical model reproduces the noise for both small and large g/γ, these limits are quite different in nature. For large g, the Lindblad jumps provide the bottleneck for transport and, thus, determine the average current and the noise. Indeed, in this regime $p_L - p_R \simeq 0$ can be adiabatically eliminated, and the classical model reduces to a three-state model $\vec{p} = [p_0, p_L + p_R, p_D]$ (see Supplemental Material [66] for details). In this limit, coherence is suppressed and $\psi = 0$. In the limit of small g/γ, transport is dominated by the coherent tunneling, which now provides the bottleneck, but this tunneling can be captured by the perturbative rate W_{LR}. In this case, we obtain $\psi \to -2$, which also constitutes a classical limit where the ψ-KUR reduces to Eq. (1). As shown in the Appendix, since the current can be expressed as a series of conductances containing both perturbative rates and Lindblad jump rates, we find $\psi \in [-2, 0]$.

It is important to point out that the dynamical activity of the classical model differs from that of the quantum model given in Eq. (5). Indeed, the classical model implies the bound $D/J^2 \geq 1/A_{\text{cl}}$ with the dynamical activity $A_{\text{cl}} = A + (W_{LR} - \Gamma/2)(p_L + p_R)$ [see Fig. 1(a)]. The term proportional to Γ is subtracted, because dephasing jumps contribute to the dynamical activity of the quantum model but not in the classical rate equation. Nonetheless, for small Γ, in the regimes where the DQD behaves classically, the quantity A is the relevant quantity that bounds the signal-to-noise ratio according to Eq. (1). For small g/γ the contribution from W_{LR} is negligible, and $A_{\text{cl}} \simeq A$. For large g/γ, interdot transitions are very rapid but do not influence the noise. As mentioned above, the relevant classical dynamics may be described by a coarse-grained three-state model. The dynamical activity of this model, A_{ad}, tends to A for large g/γ [see Fig. 1(a)]. Therefore, in the regimes where D is captured by the classical model, the ψ-KUR in Eq. (2) provides the relevant bound for the signal-to-noise ratio. We note that, in contrast to the ψ-KUR, the KUR in Eq. (9) becomes very loose as g/γ becomes large as the denominator on the right-hand side approaches A_{cl}. We note that Eqs. (2) and (9) can be combined to obtain a tighter bound.

Diffusive charge measurement—We consider next the diffusive measurements of the charge difference between the dots, which can be implemented using a quantum point contact [22,45,69,70]. The resulting diffusive current is $J_{\text{d}} = \sqrt{2\Gamma}\text{Tr}[(\hat{c}_L^\dagger \hat{c}_L - \hat{c}_R^\dagger \hat{c}_R)\hat{\rho}]$, where we assumed that all dephasing in Eq. (11) is due to the measurement. The ψ-KUR is illustrated in Fig. 1(c), where now

$$\psi = \frac{8g^2(\gamma_L + \gamma_R)}{4g^2(\gamma_L + \gamma_R) + \gamma_L\gamma_R(\gamma_L + \gamma_R + 2\Gamma)}. \quad (17)$$

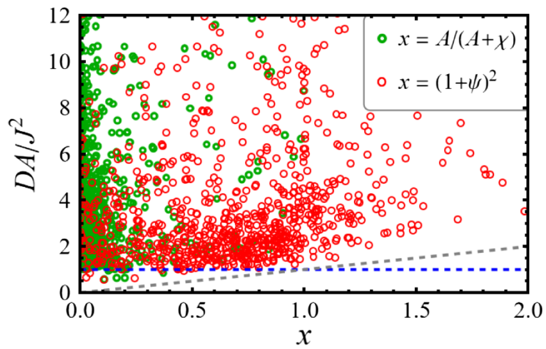

FIG. 2. A scatter plot of DA/J^2 against $(1+\psi)^2$ (red circles) and $A/(A+\chi)$ (green circles) for 1000 random networks of a five-level quantum system. Each transition $|n\rangle \leftrightarrow |k\rangle$ is either coherently or dissipatively connected. Coherent tunneling strength $g_{nk} = g_{kn}$ and jumping rates γ_{nk} are sampled from a uniform $U[0,3]$, whereas $\gamma_{kn} = \gamma_{nk}e^{-\sigma_{nk}}$, with σ_{nk} sampled from $U[3,5]$. The current is defined along a single edge with antisymmetric weights ± 1. The gray dashed line represents x, i.e., the ψ-KUR bound in Eq. (2) for red circles and the bound in Eq. (9) for green circles. The blue dashed line is 1, i.e., the classical KUR bound in Eq. (1).

In this case $\psi > 0$ always, resulting in a tighter bound than the KUR [i.e., no violations of Eq. (1) are allowed]. One of the key features of the ψ-KUR is that it is unraveling dependent. For instance, we can contrast our result with the quantum bound in Eq. (9) (green line), which exhibits opposite behavior when compared to Eq. (2), thus representing a looser constraint on the noise-to-signal ratio. Interestingly, diffusive charge measurement is not the only example where we find $\psi > 0$. It happens also for the jump current, where we count only electrons entering the system from the left reservoir, which corresponds to the current $J = \gamma_L f_L \text{Tr}\{\hat{c}_L^\dagger \hat{\rho} \hat{c}_L\}$ (see Supplemental Material [66]).

Random network of states—To illustrate the ψ-KUR in more general settings, we numerically investigate a five-level system, where each transition $|n\rangle \leftrightarrow |k\rangle$ between the computational basis states is realized either by a coherent interaction $g_{nk}|n\rangle\langle k|$ or jump operators $\sqrt{\gamma_{nk}}|n\rangle\langle k|$ and $\sqrt{\gamma_{kn}}|k\rangle\langle n|$. Values of $g_{nk} = g_{kn}$ and γ_{nk} are randomly sampled from a uniform distribution $U[0,3]$, whereas $\gamma_{kn} = \gamma_{nk}e^{-\sigma_{nk}}$, with σ_{nk} sampled form $U[3,5]$ to ensure a strong bias. We consider an antisymmetric current for a single transition $|0\rangle \leftrightarrow |1\rangle$, meaning that $\sqrt{\gamma_{10}}|1\rangle\langle 0|$ and $\sqrt{\gamma_{01}}|0\rangle\langle 1|$ have weights 1 and -1, respectively, whereas all other jumps are not counted toward the current.

The red circles in Fig. 2 show DA/J^2 vs $(1+\psi)^2$ for 1000 randomly sampled networks. These points illustrate that the factor ψ may be both positive and negative, and that the ψ-KUR provides a relevant bound also for more complex systems. The green circles show DA/J^2 vs $A/(A+\chi)$ for the same network. It is noteworthy that many green circles fall close to $x = 0$, where Eq. (9) reduces to the trivial bound $DA/J^2 \geq 0$.

Conclusions and outlook—We derived an unraveling-dependent quantum KUR that holds for Markovian open quantum systems in the steady state, and includes a factor (ψ) that captures the effect of energetic coherence in the density matrix. This bound pinpoints precisely how coherence may or may not allow for violations of the classical KUR. The physical significance of our results is substantiated by illustrating the KUR and the meaning of ψ on the DQD with with two different unravelings corresponding to different measurements. Interesting future questions include deriving thermokinetic uncertainty relations under strong system-environment couplings or for a unitary description of system and environment, investigating the transient regime [49,71,72], extending the results to the first passage times [49,73], exploring the implications of our findings on the precision of clocks [52,74,75], and generalizing a newly established clock uncertainty relation [76,77], which constitutes a generally tighter bound than the classical KUR with the average residual time in place of the dynamical activity, to the quantum regime. Since there is a growing interest in current fluctuations in non-Markovian settings [78,79], with a potential development of a theory of unravelings in non-Markovian master equations [80], our methods could be useful to find similar bounds on the signal-to-noise ratio.

Acknowledgments—P. P. P. and K. P. acknowledge funding from the Swiss National Science Foundation (Eccellenza Professorial Fellowship PCEFP2_194268).

[1] A. Streltsov, G. Adesso, and M. B. Plenio, Colloquium: Quantum coherence as a resource, Rev. Mod. Phys. **89**, 041003 (2017).
[2] R. Horodecki, P. Horodecki, M. Horodecki, and K. Horodecki, Quantum entanglement, Rev. Mod. Phys. **81**, 865 (2009).
[3] N. Brunner, D. Cavalcanti, S. Pironio, V. Scarani, and S. Wehner, Bell nonlocality, Rev. Mod. Phys. **86**, 419 (2014).
[4] K. Prech, P. Johansson, E. Nyholm, G. T. Landi, C. Verdozzi, P. Samuelsson, and P. P. Potts, Entanglement and thermokinetic uncertainty relations in coherent mesoscopic transport, Phys. Rev. Res. **5**, 023155 (2023).
[5] G. Kießlich, P. Samuelsson, A. Wacker, and E. Schöll, Counting statistics and decoherence in coupled quantum dots, Phys. Rev. B **73**, 033312 (2006).
[6] K. Ptaszyński, Coherence-enhanced constancy of a quantum thermoelectric generator, Phys. Rev. B **98**, 085425 (2018).
[7] C. L. Latune, I. Sinayskiy, and F. Petruccione, Negative contributions to entropy production induced by quantum coherences, Phys. Rev. A **102**, 042220 (2020).
[8] M. Scandi, H. J. D. Miller, J. Anders, and M. Perarnau-Llobet, Quantum work statistics close to equilibrium, Phys. Rev. Res. **2**, 023377 (2020).
[9] H. Tajima and K. Funo, Superconducting-like heat current: Effective cancellation of current-dissipation trade-off by quantum coherence, Phys. Rev. Lett. **127**, 190604 (2021).
[10] G. Francica, J. Goold, and F. Plastina, Role of coherence in the nonequilibrium thermodynamics of quantum systems, Phys. Rev. E **99**, 042105 (2019).
[11] J. P. Santos, L. C. Céleri, G. T. Landi, and M. Paternostro, The role of quantum coherence in non-equilibrium entropy production, npj Quantum Inf. **5**, 23 (2019).
[12] G. T. Landi and M. Paternostro, Irreversible entropy production: From classical to quantum, Rev. Mod. Phys. **93**, 035008 (2021).
[13] F. Rodrigues and E. Lutz, Nonequilibrium thermodynamics of quantum coherence beyond linear response, Commun. Phys. **7** (2024).
[14] J. Kurchan, A quantum fluctuation theorem, arXiv:cond-mat/0007360.
[15] H. Tasaki, Jarzynski relations for quantum systems and some applications, arXiv:cond-mat/0009244.
[16] P. Talkner, E. Lutz, and P. Hänggi, Fluctuation theorems: Work is not an observable, Phys. Rev. E **75**, 050102(R) (2007).
[17] M. Esposito, U. Harbola, and S. Mukamel, Nonequilibrium fluctuations, fluctuation theorems, and counting statistics in quantum systems, Rev. Mod. Phys. **81**, 1665 (2009).
[18] M. Campisi, P. Hänggi, and P. Talkner, Colloquium: Quantum fluctuation relations: Foundations and applications, Rev. Mod. Phys. **83**, 771 (2011).
[19] G. Manzano, J. M. Horowitz, and J. M. R. Parrondo, Quantum fluctuation theorems for arbitrary environments: Adiabatic and nonadiabatic entropy production, Phys. Rev. X **8**, 031037 (2018).
[20] K. Prech and P. P. Potts, Quantum fluctuation theorem for arbitrary measurement and feedback schemes, Phys. Rev. Lett. **133**, 140401 (2024).
[21] T. Yada, N. Yoshioka, and T. Sagawa, Quantum fluctuation theorem under quantum jumps with continuous measurement and feedback, Phys. Rev. Lett. **128**, 170601 (2022).
[22] G. T. Landi, M. J. Kewming, M. T. Mitchison, and P. P. Potts, Current fluctuations in open quantum systems: Bridging the gap between quantum continuous measurements and full counting statistics, PRX Quantum **5**, 020201 (2024).
[23] I. D. Terlizzi and M. Baiesi, Kinetic uncertainty relation, J. Phys. A **52**, 02LT03 (2018).
[24] J. P. Garrahan, Simple bounds on fluctuations and uncertainty relations for first-passage times of counting observables, Phys. Rev. E **95**, 032134 (2017).
[25] T. R. Gingrich, J. M. Horowitz, N. Perunov, and J. L. England, Dissipation bounds all steady-state current fluctuations, Phys. Rev. Lett. **116**, 120601 (2016).
[26] A. C. Barato and U. Seifert, Thermodynamic uncertainty relation for biomolecular processes, Phys. Rev. Lett. **114**, 158101 (2015).
[27] J. M. Horowitz and T. R. Gingrich, Thermodynamic uncertainty relations constrain non-equilibrium fluctuations, Nat. Phys. **16**, 15 (2020).
[28] P. P. Potts and P. Samuelsson, Thermodynamic uncertainty relations including measurement and feedback, Phys. Rev. E **100**, 052137 (2019).
[29] K. Macieszczak, K. Brandner, and J. P. Garrahan, Unified thermodynamic uncertainty relations in linear response, Phys. Rev. Lett. **121**, 130601 (2018).

[30] P. Pietzonka, F. Ritort, and U. Seifert, Finite-time generalization of the thermodynamic uncertainty relation, Phys. Rev. E **96**, 012101 (2017).

[31] J. M. Horowitz and T. R. Gingrich, Proof of the finite-time thermodynamic uncertainty relation for steady-state currents, Phys. Rev. E **96**, 020103(R) (2017).

[32] T. Koyuk and U. Seifert, Thermodynamic uncertainty relation for time-dependent driving, Phys. Rev. Lett. **125**, 260604 (2020).

[33] V. T. Vo, T. V. Vu, and Y. Hasegawa, Unified thermodynamic–kinetic uncertainty relation, J. Phys. A **55**, 405004 (2022).

[34] K. Liu, Z. Gong, and M. Ueda, Thermodynamic uncertainty relation for arbitrary initial states, Phys. Rev. Lett. **125**, 140602 (2020).

[35] Y. Hasegawa and T. Van Vu, Uncertainty relations in stochastic processes: An information inequality approach, Phys. Rev. E **99**, 062126 (2019).

[36] A. M. Timpanaro, G. Guarnieri, J. Goold, and G. T. Landi, Thermodynamic uncertainty relations from exchange fluctuation theorems, Phys. Rev. Lett. **123**, 090604 (2019).

[37] C. Maes, Frenesy: Time-symmetric dynamical activity in nonequilibria, Phys. Rep. **850**, 1 (2020), frenesy: time-symmetric dynamical activity in nonequilibria.

[38] B. K. Agarwalla and D. Segal, Assessing the validity of the thermodynamic uncertainty relation in quantum systems, Phys. Rev. B **98**, 155438 (2018).

[39] A. A. S. Kalaee, A. Wacker, and P. P. Potts, Violating the thermodynamic uncertainty relation in the three-level maser, Phys. Rev. E **104**, L012103 (2021).

[40] A. Rignon-Bret, G. Guarnieri, J. Goold, and M. T. Mitchison, Thermodynamics of precision in quantum nanomachines, Phys. Rev. E **103**, 012133 (2021).

[41] J. Liu and D. Segal, Coherences and the thermodynamic uncertainty relation: Insights from quantum absorption refrigerators, Phys. Rev. E **103**, 032138 (2021).

[42] M. Gerry and D. Segal, Absence and recovery of cost-precision tradeoff relations in quantum transport, Phys. Rev. B **105**, 155401 (2022).

[43] M. Gerry and D. Segal, Full counting statistics and coherences: Fluctuation symmetry in heat transport with the unified quantum master equation, Phys. Rev. E **107**, 054115 (2023).

[44] M. Janovitch, M. Brunelli, and P. P. Potts, Wave-particle duality in a quantum heat engine, Phys. Rev. Res. **5**, L042007 (2023).

[45] L. P. Bettmann, M. J. Kewming, and J. Goold, Thermodynamics of a continuously monitored double-quantum-dot heat engine in the repeated interactions framework, Phys. Rev. E **107**, 044102 (2023).

[46] L. M. Cangemi, V. Cataudella, G. Benenti, M. Sassetti, and G. De Filippis, Violation of thermodynamics uncertainty relations in a periodically driven work-to-work converter from weak to strong dissipation, Phys. Rev. B **102**, 165418 (2020).

[47] P. Menczel, E. Loisa, K. Brandner, and C. Flindt, Thermodynamic uncertainty relations for coherently driven open quantum systems, J. Phys. A **54**, 314002 (2021).

[48] Y. Hasegawa, Quantum thermodynamic uncertainty relation for continuous measurement, Phys. Rev. Lett. **125**, 050601 (2020).

[49] T. Van Vu and K. Saito, Thermodynamics of precision in Markovian open quantum dynamics, Phys. Rev. Lett. **128**, 140602 (2022).

[50] G. Guarnieri, G. T. Landi, S. R. Clark, and J. Goold, Thermodynamics of precision in quantum nonequilibrium steady states, Phys. Rev. Res. **1**, 033021 (2019).

[51] F. Carollo, R. L. Jack, and J. P. Garrahan, Unraveling the large deviation statistics of Markovian open quantum systems, Phys. Rev. Lett. **122**, 130605 (2019).

[52] P. Erker, M. T. Mitchison, R. Silva, M. P. Woods, N. Brunner, and M. Huber, Autonomous quantum clocks: Does thermodynamics limit our ability to measure time?, Phys. Rev. X **7**, 031022 (2017).

[53] Y. Hasegawa, Thermodynamic uncertainty relation for general open quantum systems, Phys. Rev. Lett. **126**, 010602 (2021).

[54] Y. Hasegawa, Irreversibility, Loschmidt echo, and thermodynamic uncertainty relation, Phys. Rev. Lett. **127**, 240602 (2021).

[55] H. J. D. Miller, M. H. Mohammady, M. Perarnau-Llobet, and G. Guarnieri, Thermodynamic uncertainty relation in slowly driven quantum heat engines, Phys. Rev. Lett. **126**, 210603 (2021).

[56] Y. Hasegawa, Thermodynamic uncertainty relation for quantum first-passage processes, Phys. Rev. E **105**, 044127 (2022).

[57] Y. Hasegawa, Quantum thermodynamic uncertainty relation under feedback control, arXiv:2312.07407.

[58] H. Carmichael, An open systems approach to quantum optics, *Lect. Notes Phys.Monogr.,* 10.1007/978-3-540-47620-7 (1993).

[59] K. Jacobs, *Quantum Measurement Theory and its Applications* (Cambridge University Press, Cambridge, England, 2014).

[60] W. G. van der Wiel, S. De Franceschi, J. M. Elzerman, T. Fujisawa, S. Tarucha, and L. P. Kouwenhoven, Electron transport through double quantum dots, Rev. Mod. Phys. **75**, 1 (2002).

[61] H.-P. Breuer and F. Petruccione, *The Theory of Open Quantum Systems* (Oxford University Press, Oxford, 2003).

[62] P. P. Potts, A. A. S. Kalaee, and A. Wacker, A thermodynamically consistent Markovian master equation beyond the secular approximation, New J. Phys. **23**, 123013 (2021).

[63] M. B. Plenio and P. L. Knight, The quantum-jump approach to dissipative dynamics in quantum optics, Rev. Mod. Phys. **70**, 101 (1998).

[64] G. Schaller, *Open Quantum Systems Far from Equilibrium* (Springer, Cham, 2013), Vol. 881, 10.1007/978-3-319-03877-3.

[65] D. Mandal and C. Jarzynski, Analysis of slow transitions between nonequilibrium steady states, J. Stat. Mech. (2016) 063204.

[66] See Supplemental Material at http://link.aps.org/supplemental/10.1103/PhysRevLett.134.020401 for details of derivation of ψ-KUR, the expression for χ, detailed calculations for the double quantum dot example, specifics

of the scatter plot, and an additional example of a coherently driven qubit.
[67] T. Baumgratz, M. Cramer, and M. B. Plenio, Quantifying coherence, Phys. Rev. Lett. **113**, 140401 (2014).
[68] M. T. Mitchison, M. P. Woods, J. Prior, and M. Huber, Coherence-assisted single-shot cooling by quantum absorption refrigerators, New J. Phys. **17**, 115013 (2015).
[69] H.-S. Goan, G. J. Milburn, H. M. Wiseman, and H. Bi Sun, Continuous quantum measurement of two coupled quantum dots using a point contact: A quantum trajectory approach, Phys. Rev. B **63**, 125326 (2001).
[70] S. A. Gurvitz, Measurements with a noninvasive detector and dephasing mechanism, Phys. Rev. B **56**, 15215 (1997).
[71] G. Blasi, S. Khandelwal, and G. Haack, Exact finite-time correlation functions for multiterminal setups: Connecting theoretical frameworks for quantum transport and thermodynamics, Phys. Rev. Res. **6**, 043091 (2024).
[72] J. Bourgeois, G. Blasi, S. Khandelwal, and G. Haack, Finite-time dynamics of an entanglement engine: Current, fluctuations and kinetic uncertainty relations, Entropy **26**, 497 (2024).
[73] M. J. Kewming, A. Kiely, S. Campbell, and G. T. Landi, First passage times for continuous quantum measurement currents, Phys. Rev. A **109**, L050202 (2024).
[74] F. Meier, E. Schwarzhans, P. Erker, and M. Huber, Fundamental accuracy-resolution trade-off for timekeeping devices, Phys. Rev. Lett. **131**, 220201 (2023).
[75] O. Culhane, M. J. Kewming, A. Silva, J. Goold, and M. T. Mitchison, Powering an autonomous clock with quantum electromechanics, New J. Phys. **26**, 023047 (2024).
[76] K. Prech, G. T. Landi, F. Meier, N. Nurgalieva, P. P. Potts, R. Silva, and M. T. Mitchison, Optimal time estimation and the clock uncertainty relation for stochastic processes, arXiv:2406.19450.
[77] K. Macieszczak, Ultimate kinetic uncertainty relation and optimal performance of stochastic clocks, arXiv:2407.09839.
[78] M. Brenes, G. Guarnieri, A. Purkayastha, J. Eisert, D. Segal, and G. Landi, Particle current statistics in driven mesoscale conductors, Phys. Rev. B **108**, L081119 (2023).
[79] L. P. Bettmann, M. J. Kewming, G. T. Landi, J. Goold, and M. T. Mitchison, Quantum stochastic thermodynamics in the mesoscopic-leads formulation, arXiv:2404.06426.
[80] X. Li, S.-X. Lyu, Y. Wang, R.-X. Xu, X. Zheng, and Y. J. Yan, Toward quantum simulation of non-Markovian open quantum dynamics: A universal and compact theory, Phys. Rev. A **110**, 032620 (2024).
[81] C. W. Helstrom, Quantum detection and estimation theory, J. Stat. Phys. **1**, 231 (1969).
[82] M. Hotta and M. Ozawa, Quantum estimation by local observables, Phys. Rev. A **70**, 022327 (2004).
[83] S. Gammelmark and K. Mølmer, Fisher information and the quantum Cramér-Rao sensitivity limit of continuous measurements, Phys. Rev. Lett. **112**, 170401 (2014).

End Matter

Appendix: Derivation of Eq. (2)—To derive the ψ-KUR given in Eq. (2), we consider the following deformation of the jump operators in the Lindblad master equation [Eq. (3)]: $\hat{L}_k \to \hat{L}_{k,\theta} \coloneqq \sqrt{1+\theta}\hat{L}_k$. This results in the modified Lindblad master equation

$$\frac{d}{dt}\hat{\rho}_t = -i[\hat{H},\hat{\rho}_t] + (1+\theta)\sum_k D[\hat{L}_k]\hat{\rho} \eqqcolon \mathcal{L}_\theta\hat{\rho}_t, \tag{A1}$$

such that we recover the original master equation when $\theta \to 0$. Contrary to the method used to derive Eq. (9), here the deformation is only in the jump operators. It, therefore, does not amount to a homogeneous scaling of time. We use a generalized quantum Cramér–Rao bound [81,82]

$$\mathrm{Var}_\theta[N(\tau)]_{\theta=0} \geqslant \frac{\{\partial_\theta \mathrm{E}_\theta[N(\tau)]_{\theta=0}\}^2}{\mathcal{I}(\theta\to 0)}, \tag{A2}$$

where $\mathrm{E}_\theta[N(\tau)]$ and $\mathrm{Var}_\theta[N(\tau)]$ denote the expectation value and the variance of $N(\tau)$ corresponding to the distorted dynamics [Eq. (A1)], and $\mathcal{I}(\theta)$ is the quantum Fisher information (QFI) of the parameter θ. In Eq. (A2), $N(\tau)$ plays the role of an estimator for the parameter θ. While it may not be a good estimator (it is generally biased), it nevertheless is a possible estimator and, thus, obeys the Cramér–Rao bound. While Eq. (A2) holds universally, analytically computing all expressions therein is often not straightforward, as evidenced by this Letter. Similarly, finding measurements that saturate it is highly nontrivial.

Using the formalism of Ref. [83] to compute the QFI of continuously monitored open quantum systems, we find

$$\mathcal{I}(\theta\to 0) = \tau A. \tag{A3}$$

The expectation value of the time-integrated current is given by

$$\mathrm{E}_\theta[N(\tau)] = \begin{cases} (1+\theta)\int_0^\tau dt \mathrm{Tr}\{\mathcal{J}e^{\mathcal{L}_\theta\tau}\hat{\rho}\} & \text{(jump current)} \\ \sqrt{1+\theta}\int_0^\tau dt \mathrm{Tr}\{\mathcal{J}e^{\mathcal{L}_\theta\tau}\hat{\rho}\} & \text{(diffusive current).} \end{cases} \tag{A4}$$

Due to a different prefactor, we obtain two expressions for its partial derivative with respect to θ:

$$\partial_\theta \mathrm{E}_\theta[N(\tau)]_{\theta=0} = \begin{cases} J\tau(1+\psi) & \text{(jump current)} \\ J\tau\left(\frac{1}{2}+\psi\right) & \text{(diffusive current)} \end{cases}. \tag{A5}$$

Using the relation $\mathrm{Var}_\theta[N(\tau)]_{\theta=0} = D\tau$ and inserting Eqs. (A3) and (A5) into the quantum Cramér–Rao bound [Eq. (A2)] leads to our ψ-KUR [Eq. (2)]. See Supplemental Material [66] for a derivation of Eqs. (A3) and (A5).

The classical KUR [Eq. (1)] can be recovered in the limit of incoherent dynamics as a result of $[\hat{H}, \hat{\rho}] = 0$, implying $\psi = 0$. For the DQD, this is what happens in the limit $g \to \infty$. As discussed in the main text, we may also recover $(1+\psi)^2 = 1$ when $\psi = -2$, which happens for the DQD in the limit $g \to 0$ where both $[\hat{H}, \hat{\rho}]$ as well as J tend to zero, c.f. Eq. (13). This observation may be understood by considering the rates in the classical model. In the limit of large g, the couplings to the bath become the bottleneck that dominates transport, and the current reduces to $J = \gamma_L\gamma_R(f_L - f_R)/(\gamma_L + \gamma_R)$. Under the rescaling in Eq. (A1), $\mathrm{E}_\theta[N(\tau)] = J\tau(1+\theta)$, which results in $\psi = 0$ from Eq. (A5). In contrast, in the limit of small g, interdot tunneling with rate W_{LR} provides the bottleneck and the current reduces to $J = W_{LR}(f_L - f_R)$. Since W_{LR} is inversely proportional to the Lindblad jump rates, the rescaled integrated current reduces to $\mathrm{E}_\theta[N(\tau)] = J\tau/(1+\theta) \simeq J\tau(1-\theta)$ for small θ, which results in $\psi = -2$. For arbitrary interdot couplings, the current can be written as a series of conductances

$$J = (\gamma_L^{-1} + \gamma_R^{-1} + W_{LR}^{-1})^{-1}(f_L - f_R). \tag{A6}$$

The rescaled current then reads, for small θ,

$$\mathrm{E}_\theta[N(\tau)] = J\tau\left(1 + \theta\frac{W_{LR}(\gamma_L + \gamma_R) - \gamma_L\gamma_R}{W_{LR}(\gamma_L + \gamma_R) + \gamma_L\gamma_R}\right), \tag{A7}$$

which imposes in $-2 \leq \psi \leq 0$. As we detail in Supplemental Material [66], the same restrictions for ψ hold whenever the current can be written as a series of conductances including both perturbative rates as well as Lindblad jump rates.

It is interesting to examine Eqs. (2) and (9) as a quantum Cramér–Rao bound, c.f. Eq. (A2). In Eq. (2), the quantum correction ψ arises from the numerator, i.e., the bias of the estimator. The bound becomes trivial (i.e., the right-hand side vanishes) when the estimator does not depend on θ, which happens for $\psi = -1$ [c.f. Eq. (A5)]. In this regime, where coherence plays a strong role, we can, thus, not expect our bound to be tight, as the fluctuations generally remain finite even when they do not contain information on θ. In contrast, the quantum correction χ in Eq. (9) arises from the quantum Fisher information, i.e., the denominator in Eq. (A2) [48]. The bound becomes loose when there is a large amount of information on θ in the output of the system. This generally happens when the system hosts fast processes, which allow for estimating time precisely, since in Ref. [48], θ corresponds to a rescaling of time. This explains why Eq. (9) becomes loose for large g in Fig. 1.